Analysis and Design of a Parallel Resonant Converter for Constant Current Input to Constant Voltage Output DC-DC Converter Over Wide Load Range

Tarak Saha, Hongjie Wang, Baljit Riar and Regan Zane
Department of Electrical and Computer Engineering
Utah State University, Logan, USA
E-mail: taraksaha.ee@gmail.com

***Abstract*— With long distance power distribution systems, constant current distribution is preferred over constant voltage due to robustness against cable voltage drop and cable faults. Multiple power converter modules that are connected in series in such a system either regulate their output current or voltage, as needed. With a constant current input, the input voltage of a converter is dependent on the load and this voltage varies over a wide range with the load. The design of a constant current input to constant voltage output converter is detailed in this paper. The parallel resonant converter (PRC) is proposed for this application to naturally maintain constant output voltage over a wide load range. The control method, zero voltage switching realization and design guidelines are presented. The proposed design is experimentally verified through testing of a designed PRC that regulates a constant output voltage of 120 V when connected to 1 A current source for a load range of 50 W to 450 W.**

Keywords — constant current distribution, parallel resonant converter, constant output voltage.

I. INTRODUCTION

Resonant power conversion topologies have widely been used in various applications such as DC distribution systems [1], bi-directional DC-DC converters [2], and wireless power transfer systems [3] due to their benefits of soft-switching ability, low EMI, high power density etc. For subsea DC power distribution systems, distance between a converter and power source, and distance among the converters could be very large, needing robust power distribution architecture that is immune to voltage drop along the cable and cable faults. With such a scenario, constant current distribution with sea water return is preferred over a constant voltage distribution [4-7]. Fig. 1 shows a diagram of an underwater DC distribution system where the shore based power supply drives constant current through the trunk cable and the current reaches back to the source through seawater return. Multiple DC-DC converter modules tap power from the constant current feed to regulate their output voltage or current.

In [8-9] current fed topologies are presented for converters used in subsea application. However, resonant topologies with typical current fed inverter stage increases the device ratings higher than its average DC input voltage and, thus, are not practically suitable for low-current high-voltage systems. Also, with current fed

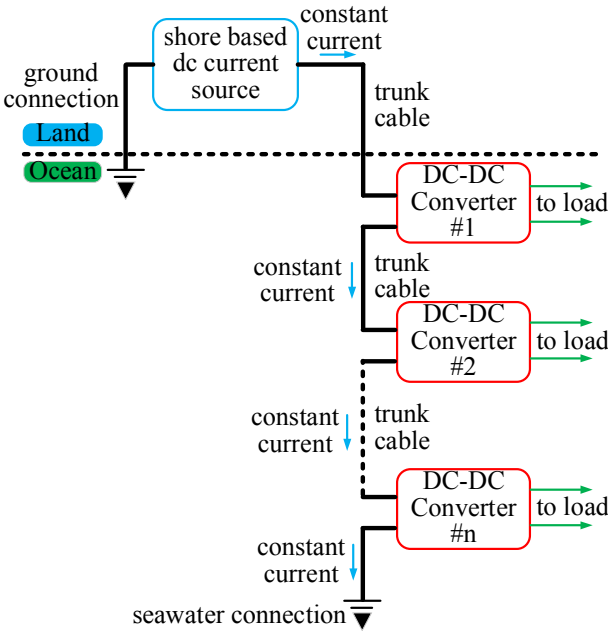

Fig. 1. Underwater DC distribution system

topologies, it is challenging to achieve zero voltage switching (ZVS) which is essential when switching with high voltages for improved efficiency and EMI. ON/OFF type of control can be employed for current fed topologies to reduce the hard switching problem but this requires a large filter at the input stage to avoid any low frequency oscillation of input voltage of the converter propagating to the source cable. Moreover, with current fed topologies, the voltage on the input side fluctuates at double the switching frequency of operation which, if not filtered adequately, can create instability through interaction with the inductance and capacitances of the submarine cable. Hence, for low constant current high voltage power distribution systems, voltage fed converter stages with input voltages that vary with load are preferred. For conventional converters with constant input voltage, there are several topologies available with detailed analysis in literature [10-12]. In [13], a parallel resonant converter (PRC) topology is presented to achieve constant current output, however the converter is operated from a constant DC voltage input. In addition, control through switching frequency variation is not preferred since it introduces additional challenges in design of input EMI filter and gate driver [14]. In [15] a series resonant converter (SRC) topology is presented

that operates as a constant DC current input to a constant DC current output converter, with voltage fed inverter stage. However, achieving constant DC voltage output from constant DC current input is not yet analyzed in the literature.

In this paper, a DC-DC PRC topology is analyzed and designed to achieve a steady state constant DC voltage output characteristics from a constant DC current input source over a wide load range. Selection of the resonant frequency to overcome the limitation on light load operation from constant DC current input is also addressed. Section II covers the basic steady state operation of the converter and derivation of steady state input/output quantities. In Section III, design of the converter, its control methodology and soft-switching realization are presented. Hardware results are shown in Section IV for a PRC, which is operated at 250 kHz from a constant input source of 1 A with its output regulated at 120 V for a load range of 50 W to 450 W, to show the behavior of the converter during steady state as well as under load transients.

II. Steady State Analysis of a PRC with a Constant Current Input

The PRC circuit topology operating from a constant current input is shown in Fig. 2(a). On the primary side of the converter, MOSFETs Q_1 – Q_4 forms the DC-AC inverting stage, which operates at DC input voltage V_{in}, with a symmetrical phase shift modulation between leg A and leg B with phase shift angle α and produces a quasi-square wave voltage (v_{AB}) at the inverter output, as shown in Fig. 2(b). The resonant tank is formed by the inductor L_r and capacitor C'_r placed on the secondary side of an n:1 isolation transformer. The voltage across the resonant capacitor is rectified and then filtered by an output filter stage formed by an inductor L_f and capacitor C_f. Input power from the constant current source I_{in} is processed by this converter to regulate the output voltage across the load (R_{load}) at a constant value of V_{out}.

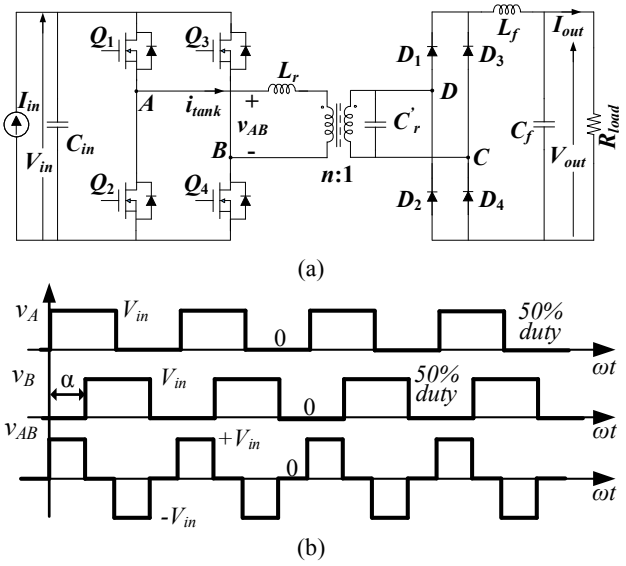

Fig. 2. PRC circuit topology with constant current input (a) and its phase shift modulation strategy (b).

The following analysis assumes that the converter is ideal without any loss. Also, it assumes that the loaded quality factor of the tank is high enough to filter out the harmonics generated from the inverter stage and the diode rectifier on the output stage operates under continuous conduction mode. With the fundamental approximation technique, the equivalent circuit of the AC stage in the PRC can be drawn as shown in Fig. 3, where the ratio of output voltage to input voltage can be given as

$$\frac{v_o}{v_{AB}} = \frac{1}{1+s\frac{L_r}{R_e}+s^2 L_r C_r} = \frac{1}{1+\frac{s}{Q\omega_o}+\frac{s^2}{\omega_o^2}}, \quad (1)$$

and the amplitude of the input voltage and output voltages are given by

$$\left|v_{AB,pk}\right| = \frac{4}{\pi}\sin(\frac{\alpha}{2})V_{in} \quad and \quad \left|v_{o,pk}\right| = \frac{n\pi}{2}V_{out}, \quad (2)$$

where, the variables used above are defined as

$$\omega_o = \frac{1}{\sqrt{L_r C_r}}, \quad C_r = \frac{C_r'}{n^2}, \quad Z_o = \sqrt{\frac{L_r}{C_r}}, \quad (3)$$

$$R_e = \frac{n^2\pi^2}{8}R_{load}, \quad Q = \frac{R_e}{Z_o}, \quad F = \frac{\omega_s}{\omega_o} = \frac{f_s}{f_o}. \quad (4)$$

Here, ω_o is the angular resonant frequency, Z_o is the characteristic impedance of the resonant tank, Q is the loaded quality factor of the tank and F is the normalized switching frequency.

With power balance from input to output of the converter, the steady state input voltage can be represented in terms of output voltage as

$$V_{in} = \frac{P_{out}}{I_{in}} = \frac{V_{out}^2}{I_{in}R_{load}}. \quad (5)$$

Substituting (2) in (1) and utilizing (5) the steady state DC output voltage can be derived as

$$V_{out} = \frac{Z_o I_{in}}{n\sin(\frac{\alpha}{2})}\sqrt{F^2+Q^2(1-F^2)^2}, \quad (6)$$

Now, if the switching frequency (f_s) of the converter is

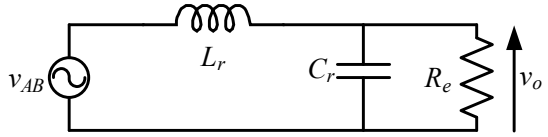

Fig. 3. Equivalent circuit of PRC with fundamental harmonic approximation

chosen to be equal to the resonant frequency (f_o) of the tank i.e. at $F = 1$, then it can be derived from (6) that the output DC voltage becomes independent of Q and as a result independent of R_{load}. The output voltage thus can be given by

$$V_{out} = \frac{Z_o I_{in}}{n \sin(\frac{\alpha}{2})}. \quad (7)$$

From (7), it can be observed that for a given input current, output voltage, transformer turns ratio and the steady state control angle α, Z_o can be easily calculated from which the tank components can be designed. In addition, it can be seen from (5), that with constant current input, the input voltage varies with load. The final expression of input voltage is given by

$$V_{in} = \frac{Z_o^2 I_{in}}{n^2 \sin^2(\frac{\alpha}{2}) R_{load}}. \quad (8)$$

The output power P_{out} of the converter for a given R_{load}, can be given by

$$P_{out} = \frac{Z_o^2 I_{in}^2}{n^2 \sin^2(\frac{\alpha}{2}) R_{load}} [F^2 + Q^2 (1 - F^2)^2]. \quad (9)$$

From (9), it should be noted that with $F = 1$, for a given load resistor R_{load}, P_{out} is minimum with $\alpha = 180°$, and P_{out} as well as V_{out} goes higher as α is reduced which is opposite of constant input voltage based PRC. It should also be noted here that operating with switching frequency equal to resonant frequency also eliminates the limitation of minimum power operation of the converter with constant current input, as discussed in [1].

III. Design of the PRC

For the converter design, the first step is to find the resonant tank components. For a given input current I_{in} and output voltage V_{out}, transformer turn ratio n, and with α chosen to be 120° the characteristic impedance Z_o of the tank can be found from (7). For a selected switching frequency, which is also the resonant frequency, the resonant tank components can be found from

$$L_r = \frac{Z_o}{\omega_o} = \frac{Z_o}{2\pi f_o}, \quad (10)$$

$$C_r = \frac{1}{\omega_o Z_o} \Rightarrow C_r' = \frac{n^2}{\omega_o Z_o}. \quad (11)$$

The resonant tank capacitor is placed at the secondary side of the transformer so that the leakage inductance of the transformer can be absorbed into the tank inductance L_r. The rms current in the tank inductor i_{Lr_rms} and rms voltage across the resonant capacitor v_{Cr_rms} are given by

$$i_{Lr\_rms} = \frac{n\pi}{2\sqrt{2}} \frac{V_{out}}{Z_o} \sqrt{1 + \frac{1}{Q^2}}, \quad (12)$$

$$v_{Cr\_rms} = \frac{\pi}{2\sqrt{2}} V_{out}. \quad (13)$$

The choice of transformer turns ratio impacts the maximum rms current in the tank current which occurs at highest load. From (7) and (12) transformer turns ratio can found out by

$$n = \frac{\frac{8}{\pi^2} \frac{V_{out} \sin(\frac{\alpha}{2})}{R_{load\_min} I_{in}}}{\sqrt{(I_{Lr\_rms\_max} \frac{2\sqrt{2}}{\pi} \frac{\sin(\frac{\alpha}{2})}{I_{in}})^2 - 1}}, \quad (14)$$

where, $I_{Lr\_rms\_max}$ is the maximum rms current in the tank inductor and R_{load_min} is the minimum load resistance, corresponding to maximum load at the output. With a design choice of $I_{Lr\_rms\_max}$, the transformer turns ratio can be optimized from (14). After determining n, resonant tank component values can be found following (7), (10) and (11).

A. Device Selection

The primary side inverter devices block voltage equal to input DC voltage V_{in} whose maximum value is decided based on the maximum load and efficiency (η) of the converter and can be found out by

$$V_{pri\_FET} \geq \frac{P_{out\_max}}{\eta I_{in}}. \quad (15)$$

The rms current rating for the MOSFETs are determined by the tank current which can be found out from (12). On the other hand, the secondary side rectifier devices see a reverse voltage equal to the peak value of voltage across resonant capacitor and thus the voltage rating for the rectifier is given by

$$V_{sec\_rect} \geq \frac{\pi V_{out}}{2}. \quad (16)$$

The average value of current through the rectifier is equal to the output current which can be easily found out from maximum load power and output voltage V_{out}.

B. Modulation for Control

It is established in Section II that the PRC behaves as a natural voltage source at its output when operated at switching frequency equal to the resonant frequency and hence a control scheme that varies the switching frequency to regulate its output cannot be employed here. It can be seen from (7) that for the designed converter, the output voltage can be controlled by the phase shift angle α and hence phase shift modulation strategy is used here.

C. ZVS Realization

Based on the analysis presented in [16, 17], for an SRC whose primary side inverter is similar in operation to the PRC, switches in the leading leg (leg A) need zero voltage switching (ZVS) assistance whereas, lagging leg (leg B) achieves ZVS by the tank current itself. As presented in [17], an active ZVS assisting circuit consisting of an auxiliary half bridge leg and ZVS assisting inductor L_{ZVS}, is used here to achieve ZVS turn ON of the MOSFETs in leg A. By controlling the phase shift angle between leg A and this auxiliary leg, ZVS assistance is controlled, over the load range.

The tank current in PRC lags the fundamental component of inverter output voltage and this angle of lagging increases with the load. This lagging phase angle can be determined from the angle of the impedance seen by the primary side inverter, at fundamental frequency, and this is expressed as

$$\begin{aligned}\angle Z_{in} &= \tan^{-1}\left(\frac{F}{Q(1-F^2)}\right) - \tan^{-1}(FQ) \\ &= \frac{\pi}{2} - \tan^{-1}(Q).\end{aligned} \tag{17}$$

If the tank impedance angle is high enough so that at the instant of rising edge of v_{AB}, value of tank current is negative, switches in the leg A will have ZVS by the tank current itself. Based on (17), this condition can be expressed as

$$\tan^{-1}(Q) < \frac{\alpha}{2}. \tag{18}$$

From (18), it can be seen that range of ZVS is high if α is high, as close to 180° as possible. But, operating with higher α limits the minimum output voltage and power capability under transient conditions as well as due to tolerance on resonant tank components [1]. A value of 120° for α is a good trade-off for design considering ZVS range as well as transient and component tolerances.

IV. Experimental Verification

A prototype PRC operating at 250 kHz has been developed with the parameters shown in Table I. The hardware setup of the PRC is shown in Fig. 4 which operates from a 1 A DC current source and is tested for a power level up to 450 W. The converter has been tested for its output voltage characteristics in steady state and transient conditions to verify its load independent, constant output voltage characteristics.

TABLE I
PARAMETERS OF PRC

Component	Value
L_r (µH)	264.6
C_r (nF)	24.5
f_s (kHz)	250
L_{ZVS} (µH)	55
I_g (A)	1
V_{out} (V)	120
P_{load} (W)	50 – 400
Transformer turn ratio n:1	4:1
Main MOSFETS (SiC)	C2M1000170D
L_f (µH)	80
C_f (µF)	2.35
Diode Bridge	GHXS020A060S-D1

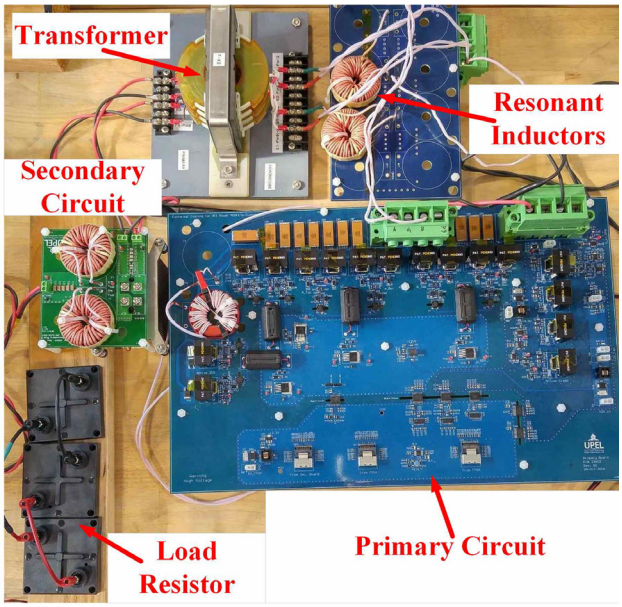

Fig. 4. Photo of the test setup.

A. Steady State Results

Hardware test results of the PRC during steady state operating conditions are shown in Fig. 5 and Fig. 6. Steady state operating waveforms of the converter are shown for α = 180° and α = 120° in fig. 5(a) and Fig. 5(b), respectively. In Fig. 5, yellow trace (CH1) is for the gate to source voltage of top MOSFET in leg A, purple (CH3) is the primary side inverter output voltage v_{AB}, green waveform (CH4) is the current in the resonant inductor and light blue trace (CH2) is the voltage across the resonant capacitor. For α = 180°, no ZVS assisting circuit is employed whereas, for α = 120°, an active ZVS assisting circuit has been used as presented in [17] and the ZVS assisting current is adjusted so that the MOSFETs in the primary side bridge achieves ZVS.

The converter has also been tested for its output characteristics by varying the load resistance (R_{load}), at two different control angle viz. minimum power operation angle α = 180° and desired operating angle α = 120°. Figure 6 shows the steady state DC output voltage (V_{out}) of the converter with respect to variation in R_{load}. In Fig. 6, the blue plot shows V_{out} vs R_{load} for

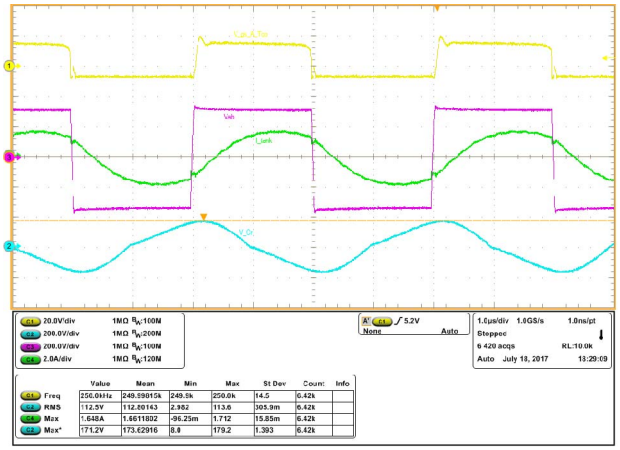

(a)

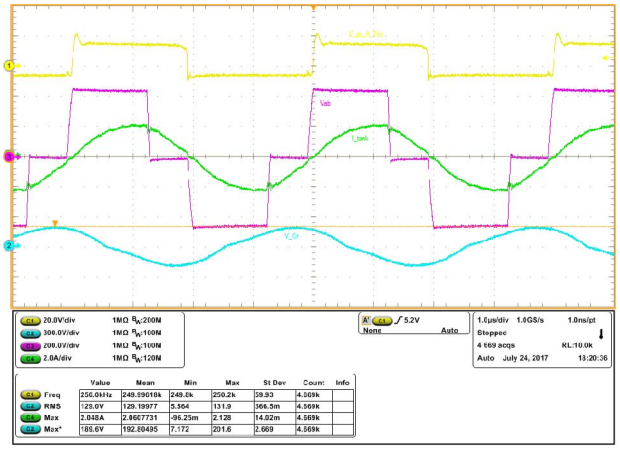

(b)

Fig. 5. PRC operating waveforms with $\alpha = 180°$ (a) and $\alpha = 120°$ (b) at $R_{load} = 34\ \Omega$. Yellow trace (CH1) is the gate to source voltage of top MOSFET in leg A, purple trace (CH3) is the primary side inverter output voltage v_{AB}, green trace (CH4) is the current in the resonant inductor and light blue (CH2) is the voltage across resonant capacitor.

$\alpha = 180°$and the red plot is for $\alpha = 120°$. It can be seen from the plots in Fig. 6, that the output voltage remains almost constant over the range of R_{load}. This shows that the converter operates as a natural voltage source at the output with a constant input current source and variable input voltage, with load. The small droop in the plots are due to series non-idealities *e.g.* ESR present in the circuit that can be easily taken care of by the closed loop controller with small variation in control angle α.

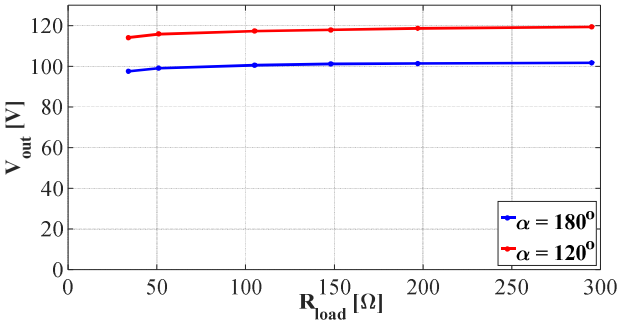

Fig. 6. Open loop output characteristics of PRC. Experimental steady state DC output voltage V_{out} v load resistance R_{load} at $\alpha = 180°$ (blue) and $\alpha = 120°$ (red)

B. Transient Results

The PRC has also been tested for transient load conditions and the results are presented in Fig. 7. For this test, the output current of the converter is changed from 1.7 A (~200 W) to 2.3 A (~275 W) and back to 1.7 A while the PRC has been operating in open loop with a fixed phase shift angle α. In Fig. 7, the blue plot (CH2) shows the DC input voltage, the green waveform (CH4) is the output load current and the DC output voltage is shown by purple trace (CH3). It can be observed from these results that the output voltage goes through overshoot or undershoot under load change transients, but settles back to its designed value of 120 V, conforming to the load independent constant output voltage characteristics.

V. CONCLUSIONS

In a constant current input DC distribution system, input voltage of a power converter varies with the load. In this paper, it is been presented how a DC-DC PRC, operating from constant current input, can be designed to achieve a steady state constant voltage output behavior across the load range. Steady state input and output quantities are derived for the converter, with fundamental harmonic approximation along with design of resonant tank components and their desired ratings. Device ratings, control methodology and soft-switching needs are also discussed here in this paper. Finally a hardware prototype has been built and tested to show that the output of the converter behaves as a constant voltage source at steady state, irrespective of load resistance. Steady state operating waveforms, with ZVS of the primary side active switches, are also shown in this paper. Simulation results under load transients also confirms the constant output voltage characteristics of the converter making it suitable for constant current input to constant voltage output converter.

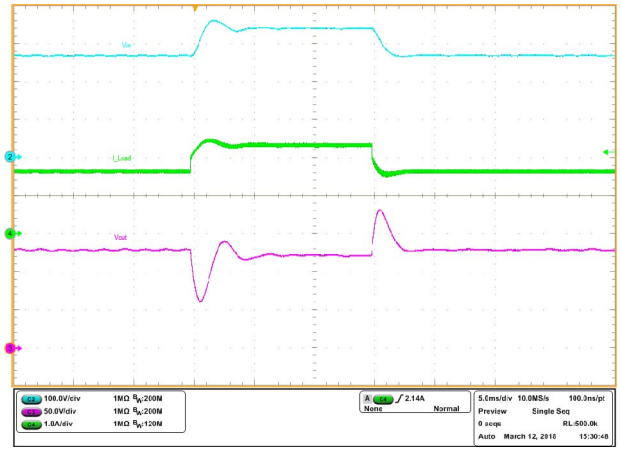

Fig. 7. Input and Output DC signals under load transient of 1.7 A (~200 W) to 2.3 A (~275 W) and back to 1.7 A, for the PRC operating in open loop. CH2 (light blue) shows the DC input voltage, CH4 (green) shows the output load current and DC output voltage is shown in CH3 (purple).

REFERENCES

[1] H. Wang, T. Saha, R. Zane, "Design Considerations for Series Resonant Converters with Constant Current Input," *2016 IEEE Energy Conversion Congress and Exposition (ECCE)*, Milwaukee, WI, 2016, pp. 1-8.

[2] L. Corradini, D. Seltzer, D. Bloomquist, R. Zane, D. Maksimovic and B. Jacobson, "Minimum Current Operation of Bidirectional Dual-Bridge Series Resonant DC/DC Converters," in *IEEE Transactions on Power Electronics*, vol.27, no.7, pp. 3266-3276, 2012.

[3] N. Hasan, H. Wang, T. Saha and Z. Pantic, "A novel position sensorless power transfer control of lumped coil-based in-motion wireless power transfer systems," *Energy Conversion Congress and Exposition (ECCE)*, pp. 586-593, Sept. 2015.

[4] K. Asakawa, J. Muramatsu, M. Aoyagi, K. Sasaki. "Feasibility study on real-time seafloor glove monitoring cable-network-power feeding system," *Underwater Technology, 2002. Proceedings of the 2002 International Symposium on*, pp. 116-122, 2002.

[5] K. Asakawa, J. Kojima, J. Muramatsu, T. Takada. "Novel current to current converter for mesh-like scientific underwater cable network-concept and preliminary test result," *OCEANS, 2003. Proceedings*, vol. 4, pp. 1868-1873, Sept. 2003.

[6] H. Wang, T. Saha and R. Zane, "Control of series connected resonant converter modules in constant current dc distribution power systems," *2016 IEEE 17th Workshop on Control and Modeling for Power Electronics (COMPEL)*, Trondheim, 2016, pp. 1-7.

[7] H. Wang, T. Saha and R. Zane, "Impedance-based stability analysis and design considerations for DC current distribution with long transmission cable," *2017 IEEE 18th Workshop on Control and Modeling for Power Electronics (COMPEL)*, Stanford, CA, 2017, pp. 1-8.

[8] A. Mohammadpour, L. Parsa, M. H. Todorovic, R. Lai, R. Datta and L. Garces, "Series-Input Parallel-Output Modular-Phase DC–DC Converter With Soft-Switching and High-Frequency Isolation," in *IEEE Transactions on Power Electronics*, vol. 31, no. 1, pp. 111-119, Jan. 2016.

[9] K. Modepalli, A. Mohammadpour, T. Li and L. Parsa, "Three-Phase Current-Fed Isolated DC–DC Converter With Zero-Current Switching," in *IEEE Transactions on Industry Applications*, vol. 53, no. 1, pp. 242-250, Jan.-Feb. 2017.

[10] S. Suzuki and T. Shimizu, "A study on efficiency improvement of high-frequency current output inverter based on immittance conversion element," *International Power Electronics Conference (IPEC-Hiroshima 2014 - ECCE ASIA)*, Hiroshima, 2014, pp. 1166-1172.

[11] H. Pollock, "Simple constant frequency constant current load-resonant power supply under variable load conditions," *in Electronics Letters*, vol. 33, no. 18, pp. 1505-1506, 28 Aug 1997.

[12] M. Borage, S. Tiwari and S. Kotaiah, "Analysis and design of an LCL-T resonant converter as a constant-current power supply," *in IEEE Transactions on Industrial Electronics*, vol. 52, no. 6, pp. 1547-1554, Dec. 2005.

[13] G. De Falco, M. Gargiulo, G. Breglio and A. Irace, "Design of a parallel resonant converter as a constant current source with microcontroller-based output current regulation control," *International Symposium on Power Electronics Power Electronics, Electrical Drives, Automation and Motion*, Sorrento, 2012, pp. 632-635.

[14] A. Safaee, P. Jain and A. Bakhshai, "Time-domain steady-state analysis of fixed-frequency series resonant converters with phase-shift modulation," *2014 IEEE Transportation Electrification Conference and Expo (ITEC)*, Dearborn, MI, 2014, pp. 1-7.

[15] H. Wang, T. Saha and R. Zane, "Analysis and design of a series resonant converter with constant current input and regulated output current," *2017 IEEE Applied Power Electronics Conference and Exposition (APEC)*, Tampa, FL, 2017, pp. 1741-1747.

[16] T. Saha, H. Wang, B. Riar and R. Zane, "Analysis of zero voltage switching requirements and passive auxiliary circuit design for DC-DC series resonant converters with constant input current," *2016 IEEE 2nd Annual Southern Power Electronics Conference (SPEC)*, Auckland, 2016, pp. 1-6.

[17] T. Saha, H. Wang and R. Zane, "Zero voltage switching assistance design for DC-DC series resonant converter with constant input current for wide load range," *2017 IEEE 18th Workshop on Control and Modeling for Power Electronics (COMPEL)*, Stanford, CA, 2017, pp. 1-5.